Iranian Journal of Materials Forming

Research Article

Effect of Fabrication Method and Porosity Content on Elastic Modulus of a Nano-Particle Dispersed Nickel Base Alloy

M.J. Hadianfard[1], R. Kavousi Heydari[1] and S.M. Arab[2*]

[1] Department of Materials Science and Engineering, School of Engineering, Shiraz University, Shiraz, Iran

[2] Department of Mechanical Engineering, University of Mohaghegh Ardabili, Ardabil, Iran

ARTICLE INFO

ABSTRACT

The change in the elastic modulus of mechanically alloyed MA754 Ni-based superalloy as a function of the porosity and fabricating method has been discussed in this study. A mixed powder of a nano-particle strengthened nickel alloy was prepared directly from its alloying elements via mechanical alloying. The mixture then consolidated using two different powder metallurgy methods, pressing was followed by sintering and as was hot extrusion followed by drawing. The powder and solid parts were characterized by XRD, XRF, and microscopic examination. The porosity content and the elastic modulus of the samples were measured via Archimedes, image analysis, tensile, and/or compression tests, respectively. The results indicated that two methods of porosity measurement provided different values for each specimen. In addition, results showed, while processing method has influences on porosity content, it also affects the elastic modulus of the alloy tremendously. Two different values of experimental modulus can be justified by the effect of texture. The different linear and polynomial models are given for different methods of the processing.

© Shiraz University, Shiraz, Iran, 2021

1. Introduction

Nano-particle strengthened superalloys, which are known as oxide dispersion strengthened (ODS), are advanced materials design to be used in high-temperature applications. These groups of materials are produced only through different methods of powder metallurgy [1, 2]. This alloy's strength relies on the higher temperatures' strength of nano-oxide particles dispersed in the nickel-chromium matrix to enhance the resistance against creep rupture by dislocation and grain boundaries pinning effect [3-5]. Powder metallurgy parts typically consist of residual pores which are distributed all around the part. The nature of the pores affects the mechanical properties of the materials [6]. The amount of the porosity, size, distribution, and even shape of the pores are important factors in determining the part's mechanical properties [7]. The characteristics of the porosity are controlled by nature, shape, size of the raw powders, and fabrication parameters such as consolidation method, temperature, and time [8, 9]. Manufacturing process plays a critical role in determining the degree of consolidation, porosity content, and also pore structure. The elastic modulus is one of the most important properties among mechanical properties, which governs load-deflection behavior of the material in the elastic's region. The elastic modulus

is very sensitive to porosity content and pore structure [10-12]. It is also reported that alloying elements and cold working affect the elastic modulus of some alloys [13-15]. The fabrication method influences the elastic modulus of powder metallurgy parts by changing the structure of the pores and also by affecting the microstructure of the matrix. The effect of fabrication parameters on the elastic modulus of an Al-Cu-Li alloy has been observed [16]. This investigation aims to make more precise image of the fabrication method on the elastic modulus of a nano-particle dispersed nickel base alloy prepared by mechanical alloying and different powder metallurgy routs.

2. Materials and Methods

2.1. Experimental procedure

In this investigation, two fabrication methods were employed to fabricate same metallic powder produced via mechanical alloying. The solid samples were formed with different porosity content by each method. The selected fabrication methods were classical powder metallurgy that consisted of powder pressing, sintering, and hot extrusion followed by wire drawing. After consolidation, some specimens from both groups experienced different amounts of cold working. Pure elemental powder of nickel, chromium, aluminum, iron, and carbon with a small amount of nano-yttria (yttrium oxide) particles were mixed via mechanical alloying. The powders were supplied by Merck. Table 1 shows the typical composition of Inconel Ma754 superalloy. The fabricated powder alloy composition is shown in Table 2. The composition of the alloy is close to the composition of Ma754 super alloy, which is an oxide dispersion strengthening nickel alloy. The base element is nickel and another significant element is chromium. Fig. 1 shows the size distribution of the yttrium oxide particles, which is obtained by analyzing transmitted electron microscopy photographs through image analyzer software, the average size of the particles was calculated at about 30 nm.

Table 1. Typical composition of Ma 754 super alloy

Component	Y_2O_3	C	Ti	Al	Fe	Cr	Ni
Ma 754 alloy	0.6	0.05	0.5	0.3	1	20	Bal.

Table 2. Composition of the fabricated powder alloy

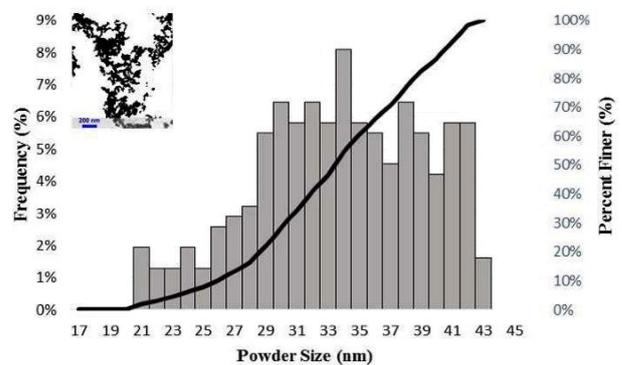| Component	Y_2O_3	C	Ti	Al	Fe	Cr	Zn	Mn	Si	Cu	Ni
Weight %	0.52	0.06	0.48	0.29	0.85	19.95	0.05	0.08	0.19	0.08	Bal.

Fig. 1. Size distribution of the yttrium oxide particles.

2.2. Powder fabrication

The alloyed powder was produced using a planetary ball mill, with a powder to ball weight ratio of 18 to 1 under a controlled atmosphere of Argon. The milling time of 24 hours was chosen for making the alloyed powder. Fig. 2 demonstrates the XRD pattern of the alloyed powder after 12 and 24 hours of milling. This figure clearly shows that the peaks of alloying elements (especially chromium) are omitted after 24 hours of milling and, the only observed peaks belongs to nickel. Fig. 3 shows the result of XRF analysis of the same powder, which indicates that the chemical composition of powder did not change after milling. The XRF analysis also shows that the other elements presented in the powder could be considered as trace elements. A combination of XRD and XRF analyses proves the formation of a solid solution phase in the Ni-based alloy. Since the mass ratio of Y_2O_3 is small (lower than 1%), XRD was not able to show its peaks, but an Yttrium' peak was observed in the XRF results.
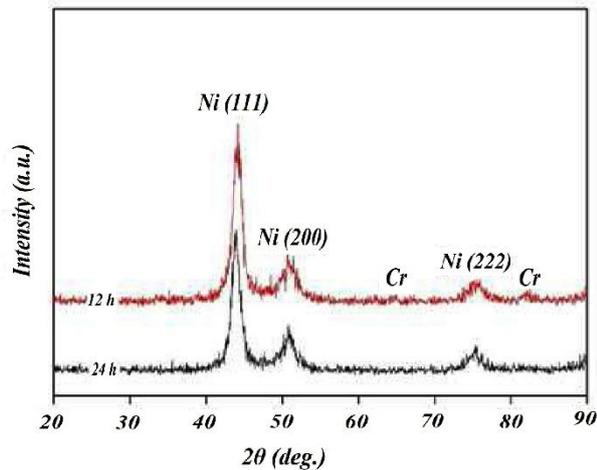
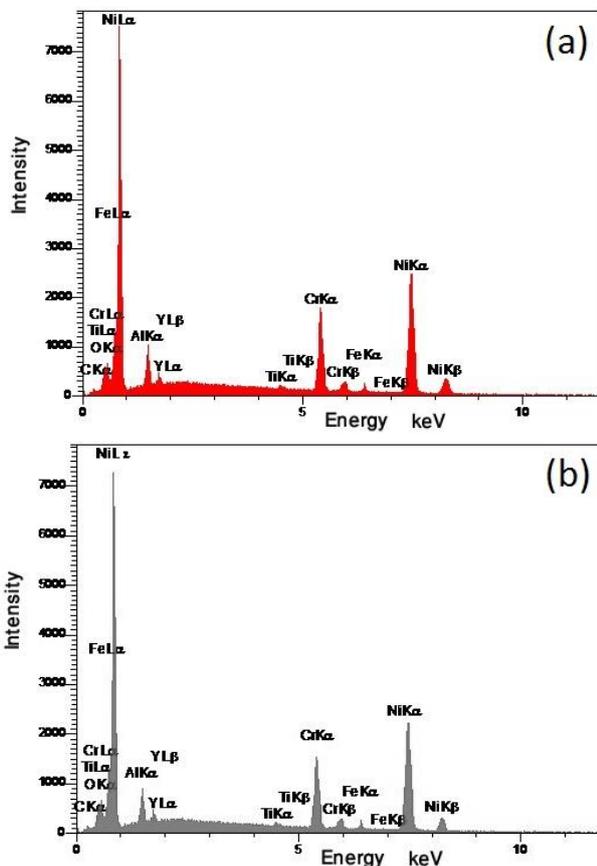**Fig. 2.** The XRD pattern of the alloyed powder after 12 and 24 hours milling.

Fig. 4. A scanning electron micrograph of the alloyed powder.

Fig. 3. Result of XRF analysis of the alloyed powder after (a) 12 h and, (b) 24 h of milling.

Fig. 5. Particle size distribution of the alloyed powder, obtained by image analysis method.

2.3. Consolidated samples fabrication

Test specimens were produced by two different methods. The first group of solid specimen was made by cold pressing and sintering (Group I). In this method, the alloyed powder was poured into a die at room temperature and pressed by a pressure of 1200 MPa before being sintered at a controlled atmosphere environment for 3 hours. In order to obtain different porosity contains, a sintering temperature of 1000 to 1250 °C was used. The second group of solid specimens was prepared through the hot extrusion method (Group II). The alloyed powder was poured into a vacuum-sealed stainless steel container, heated to a proper temperature before hot-extruding by an extrusion die with a reduction ratio of 9 to 1. Then, the steel skin was removed. Finally, the extruded samples were fed into a wire drawing machine and their cross section area was reduced 25 % at room temperature. An annealing heat treatment at 450 °C was given for 1 hour to release the residual stresses resulting from mechanical processing. Different porosity content was achieved by extruding the

Figure 4 shows the scanning electron micrograph of the alloyed powder. It is shown that the shape the particle is almost spherical and their size is in the range of 3 to 20 μm. The result of particle size analysis is presented in Fig. 5, which indicates that the average size of the powder is about 9 μm. Metallographic investigation of the powder particles showed that the consisting elements have formed a solid solution single phase.
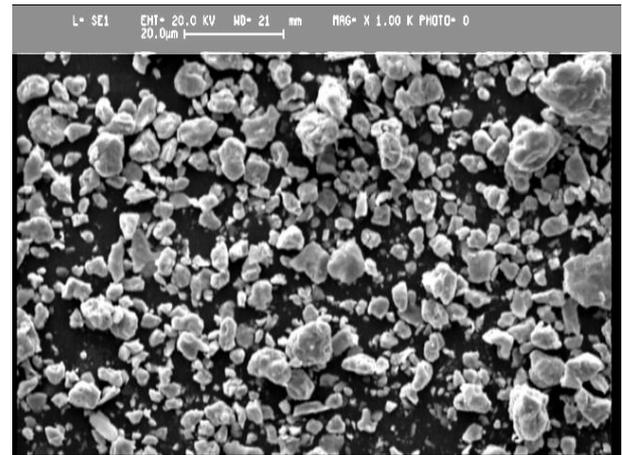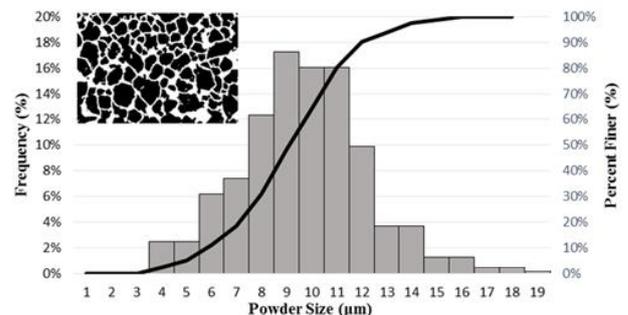
samples at temperatures of 850°C and 900°C. To reduce the porosity content (higher density) after consolidation, some specimens from both groups were cold rolled at room temperature with different reductions made in area. The fabrication method and condition of the different samples are shown in table 3.

Table 3. Fabrication method and condition of the different samples

Specimen Name	Fabrication Method	Fabrication Condition	% Cold Work after Consolidation
P1-0	Pressing +Sintering	Sintered @ 1000°C	0
P2-0	Pressing +Sintering	Sintered @ 1200°C	0
P3-0	Pressing +Sintering	Sintered @ 1250°C	0
P4-15	Pressing +Sintering	Sintered @ 1250°C	15
P5-30	Pressing +Sintering	Sintered @ 1250°C	30
E1-0	Hot Extrusion	Extrusion @ 850°C *	0
E2-0	Hot Extrusion	Extrusion @ 900°C *	0
E3-18	Hot Extrusion	Extrusion @ 900°C *	18
E4-43	Hot Extrusion	Extrusion @ 900°C *	43
E5-56	Hot Extrusion	Extrusion @ 900°C *	56
E6-67	Hot Extrusion	Extrusion @ 900°C *	67
E7-70	Hot Extrusion	Extrusion @ 900°C *	70

*Hot extrusion followed by wire drawing and annealing

2.4. Characterization methods

The density (or porosity content) was measured through two different methods; Archimedes and metallographic study followed by image analyzing. Archimedes method was employed according to ASTM C373 standard, the mass of the samples was measured carefully in dry condition and then the samples were boiled in water for 5 hours, and left in the water for another 24 hours to cool down. Finally, their floating mass was measured and the density of the samples was calculated. In the second method, two different cross-sections in the same direction from each sample were prepared and polished. The polished surfaces were investigated by an optical microscope, without etching. At least five fields on each cross section were examined.

Afterwards, total area of porosities and area of the image was measured using the software, and the occupied percent of the porosities was calculated for each photograph. An average value which obtained from all fields and for both sections of each specimen was reported as porosity content (or used to calculate the density of the samples). The modulus of elasticity was measured by mechanical methods using tensile or compression tests.

Tension tests were carried out on the samples based on the ASTM E8. The tests were carried out by speed of 0.05 cm/min, and a gauge length of 15 mm. The stress-strain curves were plotted using acquired data, and modulus of elasticity was calculated from the slope of the linear part of the stress strain curves. The compression test samples were 5mm in diameter and 6 mm in length with a length to diameter ratio of 1.2 based on ASTM E9 Standard. Both sides of a sample were fully polished, and a strip of Teflon was used on both sides of the samples to reduce friction. Compression tests were carried out by the speed of 0.2 cm/min. The modulus of elasticity was calculated according to the ASTM E111 standard, from the slope of the linear part of the stress-strain curves. Although the compression test generally gives an underestimated value of Young's modulus, the comparison of the results obtained from tensile, and compression tests on similar samples showed negligible variations between measured values. Two repeated tests were performed on each specimen, and an average value was computed for each sample. To study texture developed in extruded samples, a Rigaku Ultima IV diffractometer machine was used to investigate the general developed orientations. The Schultz method with monochromatic X-ray of Cu K_α was utilized, and data were collected for the (111) reflection of E2-0 specimens.

3. Discussion

Table 4 exhibits measured density and porosity content of each specimen obtained by Archimedes and image analyzing methods and also elastic modulus obtained from experimental studies. Figures 6 and 7 show optical micrographs of P2-0 and P4-15 samples, which are used for Image analyzing method.

Table 4. Measured density and porosity of samples

Specimen	% Relative Density (Archimedes)	% Porosity (Archimedes)	% Porosity (Image Analysis)	E (from experimental) (GPa)
P1-0	80.02	20	19.1	160
P2-0	82.01	18	10.6	169
P3-0	89.00	11	7.7	180
P4-15	93.02	7	4.8	192
P5-30	94.91	5.1	3.6	197
E1-0	89.60	10.4	7.3	129
E2-0	93.00	7	4.7	133
E3-18	94.02	5.98	4.1	135
E4-43	98.30	1.7	1.2	138
E5-56	98.90	1.1	0.8	140
E6-67	99.04	0.96	0.7	142
E7-70	99.2	0.8	0.6	143
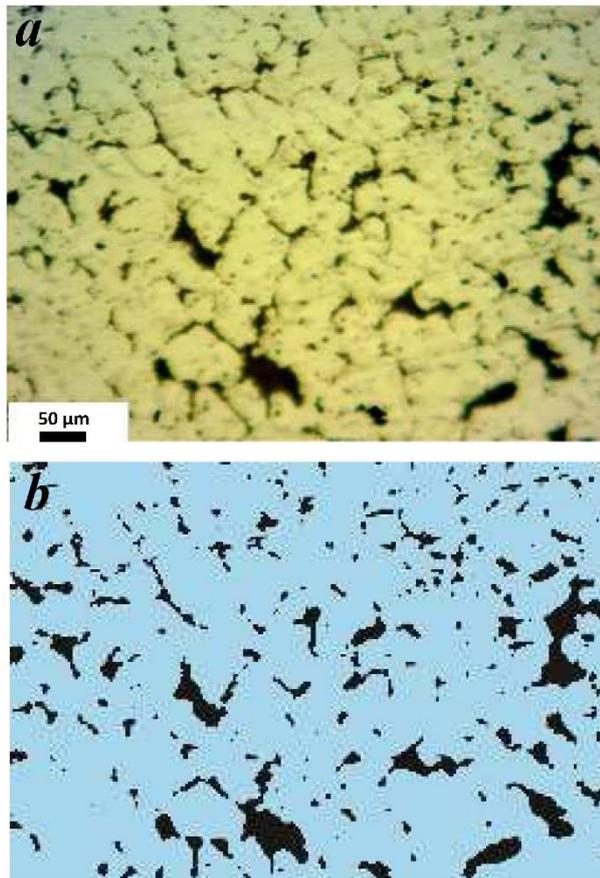
Fig. 6. An optical micrograph from longitudinal cross section of P2-0 specimen, (a) actual photograph and, (b) captured for image analyzing.

The results indicate that the porosity content in each specimen differs significantly when measured by these two various methods. In this study, porosity content measured by the image analyzing method was lower than the results obtained from Archimedes for all specimens, regardless of their porosity content or fabrication method. This difference is associated with the different basics of measurement in these two methods. While the Archimedes method measures open pores accurately, it is weak in measuring fully closed pores. However, the image analyzing method can measure both opened and closed pores at the specific cross section, whereas it may not consider tiny pores. On the other hand, the Archimedes method measures all opened and partially opened pores all over the specimens, while image analyzing considers pores only on the selected cross-sections. Since the porosity distribution is not uniform and homogeneous, the porosity content changes from one cross-section or even one field in the same cross-section to another. Therefore, increasing the number of examined cross-sections or even examined field leads to and increase in the accuracy of this method.
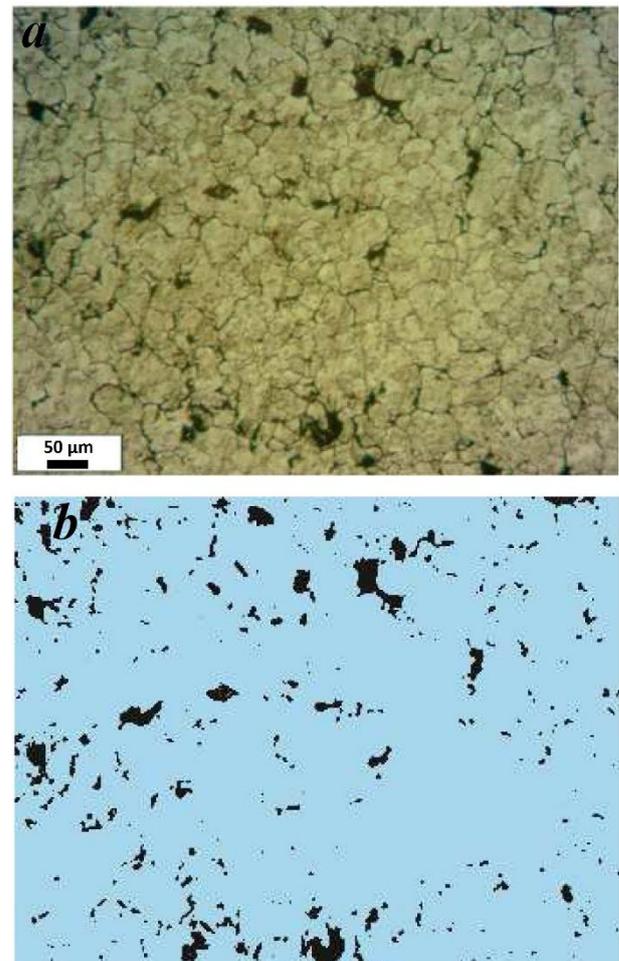
Fig. 7. An optical micrograph from longitudinal cross section of P4-15 specimen, (a) actual photograph and, (b) captured for image analyzing.

Although the difference between the two measurement methods is not large, to obtain better resolution form distinction in these two methods, normalized difference in porosity content of the samples is calculated. Fig. 8 shows normalized differences in porosity content ((porosity by the Archimedes - porosity by image)/porosity by the Archimedes) relative to the Archimedes method. While the two different groups of the samples show different porosity content, the trend of normalized differences is similar. At high densities, the variation between the two methods is small, and it increases with an increase in porosity content. At very high relative densities, pores are tiny, almost closed, and their number is meager, so they may not be recognized well using the Archimedes method due to their closed morphology, and they may hardly be distinguishable in terms of image analysis method due to their small size. Therefore, the two methods present almost the same values. At lower relative density (it is seen in the Group I), the porosity content is high and almost all pores are large and open, so they can be detected by the microscope, and also the fluid could penetrate into the pores to increase the accuracy of the Archimedes method. The two measurement methods yield similar values and the normalized differences are too small. The medium dense samples show the highest difference between the two methods, because the pores are small, and they might confuse the software in detecting the total volume percentage of the porosity. On the other hand, the fluid could penetrate the pores, which result in measuring the real values of density by the experimental method. Using two different methods showed that in high or shallow densities, both methods could be used to estimate the porosity or density, but for medium dense samples, it is preferable to use the Archimedes method.

Obtaining elastic modulus by mechanical methods is dependent on accurate measurement of displacement during the test. A small error in measuring displacement may lead to considerable change in the value of elastic modulus. Besides, the tensile test is sensitive to gripping the samples, especially in the case of weak or slippery ones. A compression test is also susceptible to friction between specimen's surfaces and compression punches. Therefore, correct preparation of the specimen and lubricity of the surfaces is essential. Another important aspect in the mechanical tests is the sample's isotropy,

which leads to different values in the anisotropic cases of different specimen's direction. Therefore, in all mechanical tests, the length of the specimens was designed in the main direction of the prior deformation.
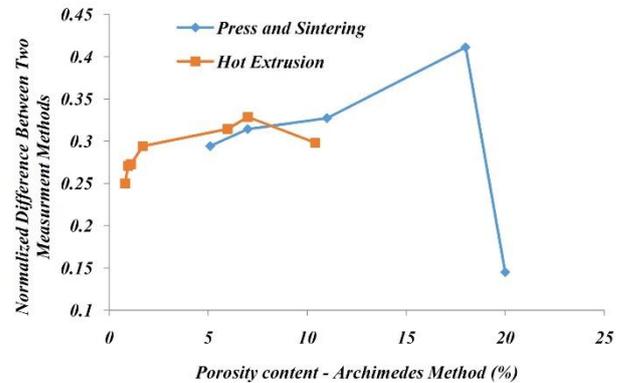

Fig. 8. Normalized differences between porosity measured by image analysis method relative to Archimedes method.

The results show that elastic modulus is very sensitive to the porosity content, and it increases by decreasing the porosity level. Fig. 9 illustrates changes in the calculated elastic modulus versus porosity content (obtained from two different methods) for Group I and II, respectively. These data show noticeable differences between the measured elastic modulus of Group I and Group II. Linear extrapolation of Archimedes data for Group I and II at full dense state gives elastic modulus of 208 GPa, and 147 GPa, respectively. Since the two groups used the same powder, which was prepared by mechanical alloying, the differences reflect the effect of the processing method on the elastic modulus of the material. These large differences may be attributed to the different mechanisms of consolidation in these two processes.
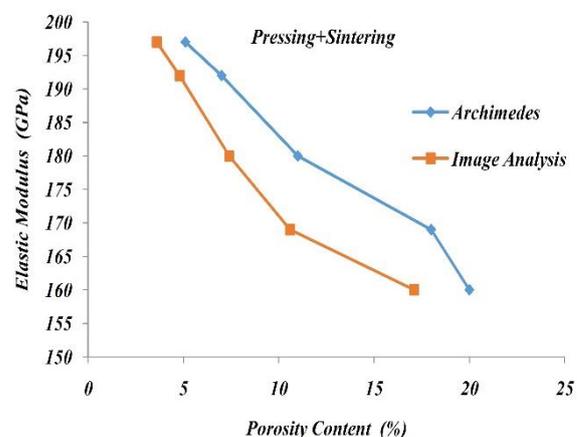

Fig. 9. The modulus of elasticity versus porosity for (a) pressed and, (b) hot extruded samples.
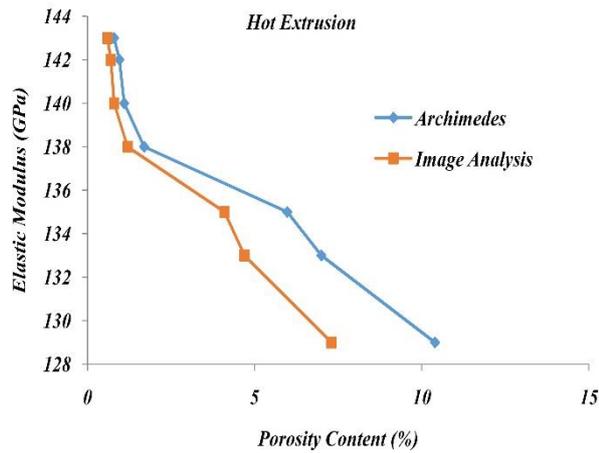
Fig. 9. Continue.

In the pressing process, friction between powder particles and also particles with surfaces of the die consumes most of the applied energy. At room temperature, plastic deformation of the superalloy powder needs a high energy due to their great toughness [17]. Therefore, particles flow to hardly fill the porosity between them. As a result, a small amount of the porosities may be eliminated during the pressing stage, and density stays relatively low. Even though powder plastic deformation in this process is small, but the deformation is almost uniform in all directions. In the sintering stage, the as-pressed powder remained at a high temperature of 1000 and 1250 $^{\circ}$C for 3 hours. This period provides sufficient time to join the particles, filling some porosities, stress-relieving the particles, and even recrystallization of some heavily deformed particles via the diffusion phenomena. Since sintering removes some effects of deformation, it may generate more isotropic grains [17]. In the hot extrusion process, powder experiences a high pressure of extrusion at high temperature of 900 $^{\circ}$C. The die pressure, with the assistance of high temperature, deforms particles easily, and fills most of the porosities. At the same time, the high temperature of the process joins the powder particles to each other and makes a solid with a lower level of porosity. On the other hand, most of the plastic deformation takes place in the direction of the extrusion. The short time of extrusion prohibits the recrystallization of heavily deformed grains. The drawing process after extrusion deeply extends the deformation of the powder particles in the drawing direction. Then grain elongation occurs in the direction of deformation, and the grain structure experiences preferred orientation [18]. The low

temperature of stress releasing heat treatment (450 $^{\circ}$C) does not afford sufficient energy for the recrystallization and keeps the grain structure unchanged.

Different values for the elastic modulus of Inconel Ma754 alloy (which are near to the present alloy) are reported, while some articles have reported values of 145-149 MPa for the elastic modulus of Ma754 [1,19,20], others have reported this value between 190 to 210 MPa [21-23]. Special Metals Corporation, USA, reported different values of 149 MPa and 203 MPa for a textured and non-textured Ma754 alloy, respectively [24]. The textured structure of Ma754 alloy, due to hot working, is reported widely [25-27]. These data indicate that the textured structure leads to lower elastic modulus and random structure provides higher elastic modulus. Therefore, it may be concluded that press and sintering method develops non-textured structure with higher elastic modulus and also higher porosity content. On the other hand, hot powder extrusion provides textured solid with lower elastic modulus and lower porosity content. Fig. 10 shows (111) pole figure of the E2-0 specimen. As is observed, the (111) planes have rotated around the normal direction (ND) towards the transverse direction (TD) and rolling direction (RD) at about 10 degrees to form β-fiber which is elongated from C component ({112} <111>) to the S component ({123} <634>) in deformed FCC structure. ({123} <634>) in deformed FCC structure.
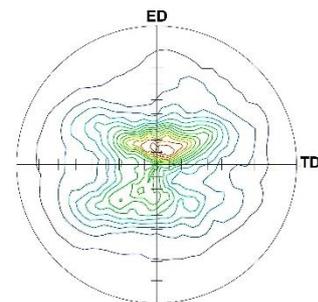
No.	Line	Level	No.	Line	Level	No.	Line	Level
1		0.314	6		1.886	11		3.458
2		0.629	7		2.201	12		3.773
3		0.943	8		2.515	13		4.087
4		1.258	9		2.829	14		4.401
5		1.572	10		3.144	15		4.716

Fig. 10. The (111) pole figure of E2-0 specimen.

In both Groups, I and II, cold-working affects the elastic modulus. An increase in the percent of cold work has increased the elastic modulus of the material. The results also show that increasing the amount of cold working leads to decrease in porosity content. Since

elastic modulus is very sensitive to the porosity content, it may be concluded that the source of an increase in elastic modulus is decreasing in porosity content. It appears cold working has moved solid materials around the pore towards its center and partly filled them. As a result of the deformation process, the volume of the individual pore has reduced, and total porosity content has decreased. On the other hand, change in the matrix properties by cold working may also affect elastic modulus. The main effect of deformation on the microstructure is increasing dislocation density due to multiplication of dislocation through Frank–Read mechanism. Moving dislocations also produce some point defects in the crystal lattice of the deformed metal [28]. These imperfections may affect elastic modulus of the material. Change in elastic modulus of some materials as a function of the cold work, has been reported [14, 29, 30]. Decrease in the elastic modulus of materials with a small amount of cold work has also been observed. It was also reported that the elastic modulus reduction, reaches a saturation level by increasing deformation [31, 32]. These observations are in contrast with the results of the current study and show that contribution of the deformed matrix, in increasing the elastic modulus of the material, is negative or negligible. Therefore, measured increase in the elastic modulus of the alloy with an increase in the amount of cold working is attributed to a reduction in porosity content by cold work. One popular method for estimation the elastic modulus of multiphase materials is using the rule of mixture. According to this rule contribution of each phase to the elastic modulus is proportional to its initial modulus and its percentage in the material [19]. For material with two phases of 1 and 2, equation 1illustrates the rule of the mixture as:

$$E = E_1 f_1 + E_2 f_2 \qquad (1)$$

where E_1 and E_2 are the elastic modulus of phase 1 and phase 2, f_1 and f_2 are the percentages of phase 1 and 2 respectively, when *f1 + f2 =100*. In this case, each specimen consists of matrix alloy and porosities. The porosities may be considered as an empty void with zero elastic modulus. In this case (a single-phase porous material) equation 1 may be simplified to equation 2:

$$E = E_0(1 - p) \qquad (2)$$

Where E, E_0, and p are the elastic modulus of the porous sample, elastic modulus of fully dense material, and percent of the porosity, respectively

This model cannot consider the effect of the fabrication method on the elastic modulus unless it considers the effect of fabrication method in the E_0 value. This way, one may consider the value of E_0 for Group I and II as 208 GPa and 147 GPa, respectively which is obtained experimentally and is consistent with the literature [19-23]. Fig. 11 shows the results of experimental and calculated elastic modulus according to the rule of mixture (equation 2) for Group I and II. As can be seen, corrected rule of mixture shows a higher value of elastic modulus compared to the experimental results for both groups. It seems effective porosities in the specimens are more extensive than measured ones, which are obtained by the Archimedes method. For the purpose of obtaining a better estimation, we may correct porosity content by using another model [10], which considers effective porosity values by multiplying experimental factors of b_i into p. Then, the value of elastic modulus is calculated according to equations 3 and 4 for pressed and hot extruded samples, respectively:

$$E = E_0(1 - bp) \qquad (3)$$
$$E = E_0(1 - b_1 p + b_2 p^2) \qquad (4)$$

The curves indicate that equation 3 and 4 have a better estimation of E than the rule of mixture for pressed and hot extruded samples, respectively. One interesting result is that the value of b_i is different for Group I and Group II (*b=1.13, b₁=1.045 and b₂=1.015*).
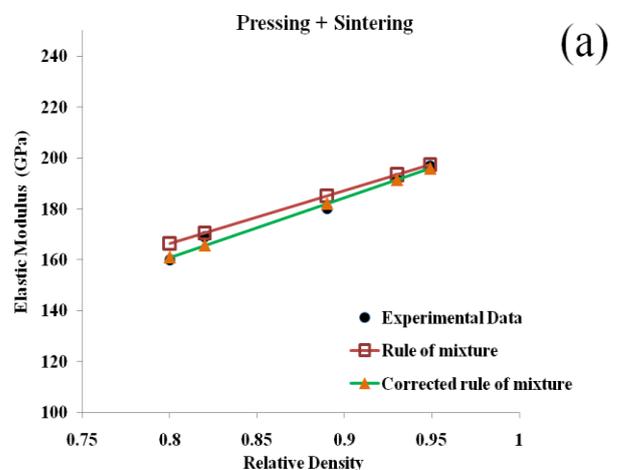

Fig. 11. Comparison between experimental and calculated elastic modulus according to the equation 2 and 3 for (a) Group I and, (b) Group II specimens.
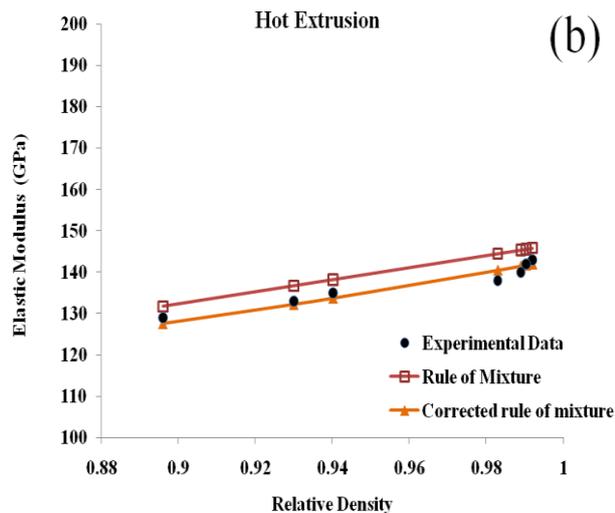
Fig. 11. Continue.

4. Conclosions

Based on the results of this study, it can be concluded that:

1- The two methods of porosity content measurement; Archimedes and image analysis, give different porosity content for the tested specimens. This difference is small in high and low densities, compared to the medium density specimens. These differences reflect the different nature measurement in these two methods.

2- Processing methods have a remarkable effect on the value of the elastic modulus of the nano-particle strengthened nickel superalloy. The large differences may be attributed to the effect of the fabrication method on the texture structure of the matrix alloy and its porosity content.

3- Elastic modulus is found to be very sensitive to the porosity content, since different processing method achieves different porosity content, fabrication method and its parameters also affect elastic modulus of the alloy through porosity content.

4- Simple rule of mixture is not suitable for the estimation of elastic modulus of the porous alloy since it cannot consider the effect of the processing method. By considering the effect of the fabrication method on the modulus of elasticity of the fully condensed alloy, one may find a better estimation of elastic modulus by using corrected rules of mixture.

5- Results indicate that the corrected rule of mixture shows a slightly higher value of elastic modulus concerning the experimental results for the tested alloy.

This could illustrate that effective porosity content is more extensive than porosity content measured via the Archimedes method. in the case of effective porosity content, the experimental correction factors b_i were used. Results showed that this correction factor is also dependant on the fabrication method.

5. References

[1] P. R. Soni, Mechanical alloying fundamentals and applications, Cambridge International Science Publishing, 2001.

[2] M. S. El-Eskandarany, Mechanical alloying for fabrication of advanced engineering materials, Noyes Publications, 2001.

[3] R. C. Reed, The Superalloys: Fundamentals and Applications, Cambridge University Press, 2006.

[4] M. J. Donachie, S. J. Donachie, Selection of Superalloys for Design, Handbook of Materials Selection, John Wiley & Sons, Inc., 2007, 293-334.

[5] C. Suryanarayana, N. Al-Aqeeli, Progress in Materials Science, 58 (2013) 383-502.

[6] N. Chawla, X. Deng, M. Marucci, K. S. Narasimhan, Effect of density on the microstructure and mechanical behavior of powder metallurgy Fe-Mo-Ni steels, *Advanced Powder Metallurgy Parts and Materials*, Edited by Metal Powder Industries Federation, Princeton, NJ, 2003.

[7] S. Parthasarathi, T. Prucher, C. J. Yu, J. Jo, R. J. Henry, Determination of dynamic elastic properties of powder metallurgy components, Review of Progress in Quantitative Nondestructive Evaluation, 12 (1993) 1631-1638.

[8] A. Salak**,** Ferrous Powder Metallurgy**,** Cambridge International Science Publishing, 1995.

[9] E. S. Huron, R. L. Casey, M. F. Henry, D.P. Mourer, The influence of alloy chemistry and powder production methods on porosity in a P/M nickel-base superalloy, Superalloys 1996, *The Minerals and Metallic Materials Society*, 1996.

[10] H. N. Yoshimura, A. L. Molisani, N. E. Narita, P. F. Cesar, H. Goldenstein, Porosity dependence of elastic constants in aluminum nitride ceramics, *Materials Research*, 10 (2007) 127-133.

[11] J. Kovacik, Correlation between elastic modulus, shear modulus, poisson's ratio and porosity in porous materials, *Advanced Engineering Materials*, 10 (2008) 250-252.

[12] A. V.Manoylov, F. M. Borodich, H. P. Evans, Modelling of elastic properties of sintered porous materials, *Proceedings of Royal Society A*, 469 (2013) 201-206.

[13] E. Salahinejad, R. Amini, M. J. Hadianfard, Contribution of nitrogen concentration to compressive elastic modulus of 18Cr–12Mn–xN austenitic stainless steels developed by powder metallurgy, *Materials and Design*, 31 (2010) 2241-2244.

[14] T. Otomo, H. Matsumoto, N. Nomura, A. Chiba, Influence of cold-working and subsequent heat-treatment on Young's modulus and strength of Co-Ni-Cr-Mo alloy, *Materials Transaction*, 51 (2010) 434-441.

[15] W. F. Druyvesteyn, B. S. Blaisse, Change in the modulus of elasticity of copper after deformation in the temperature range from 4.2-7.8 °K, *Physica* 28 (1962) 695-700.

[16] M. O' Dowd, W. Ruch, E. Starke, Dependence of elastic modulus on microstructure in 2090-type alloys, *Journal de Physique*, C3 (1987) 565-576.

[17] G. H. Gessinger, Powder metallurgy of superalloys, Elsevier Ltd, 1984.

[18] M. Levy, H. Bass, R. Stern, Handbook of Elastic Properties of Solids, Liquids, and Gases, Four-Volume Set, Academic press, 2001.

[19] S. Ochiai, Mechanical properties of metallic composites, CRC Press, 1994.

[20] Nickel Development Institute, High– temperature high – strength nickel based alloys, 393, 1995.

[21] http://www.twi-global.com/ what are the common properties of oxide dispersion strengthened ODS alloys, 2016.

[22] ASM International, Atlas of stress-strain curves 2nd ed, ASM, 2002.

[23] Pacific Northwest National Laboratory, Materials properties database for selection of high-temperature alloys and concepts of alloy design for SOFC applications, PNNL-14116, 2002.

[24] http://specialmetals.ir, Special Metals Corporation, Inconel alloy MA754, USA.

[25] J. H. Lee, K .W. Paik, L. J. Park, Y. G. Kim, J. H. Tundermann, J. J. deBarbadillo, The effect of high temperature deformation conditions on the secondary recrystallization of Ma754 plate, *Scripta Materialia*, 38 (1998) 789-794.

[26] T. R. Bieler, A. T. Mohamed, Z. Jin, M. J. Blake, The effects of hot rolling on texture and recrystallization of Ma754 sheet, *Scripta Metallurgica et Materialia*, 27 (1992) 149-154.

[27] J. Wang, W. Yuan, R. S. Mishra, I. Charit, Microstructural evolution and mechanical properties of friction stir welded ODS alloy MA754, *Journal of Nuclear Materials*, 442 (2013) 1-6.

[28] I. Kovács, L. Zsoldos, D. ter Haar, Dislocations and Plastic Deformation, Elsevier Ltd., 1973.

[29] M. Gonzalez, J. Pena, J. M. Manero, F. J. Gil, Influence of cold work in the elastic modulus of the Ti-16.2Hf-24.8Nb-1Zr alloy characterized by instrumented nanoindentation, *Key Engineering Materials*, 423 (2010) 113-118.

[30] A. Haleem, Young's modulus decrease after cold forming, Master of Science Thesis, Delft University of Technology, 2009.

[31] J. Solin, J. Alhainen, M. Chauhan, Influence of cold-work on the elastic properties of austenitic stainless steels, 7th European Stainless Steel Conference, 2011.

[32] W. Lems, The change of Young's modulus after deformation at low temperature and its recovery, Doctoral thesis, Delft University of Technology, 1963.